**A**

**DISSERTATION REPORT**

**ON**

# SIMULATION BASED STUDY OF DOUBLE GATE TUNNEL FIELD EFFECT TRANSISTOR AS A BIOSENSOR

*by*


**HEMANT CHOLA**

**2017PEV5093**


*under the supervision of*


Dr. TARUN VARMA

ASSOCIATE PROFESSOR, ECE DEPARTMENT


*Submitted in partial fulfillment for the degree of*

**MASTER OF TECHNOLOGY**

in

**VLSI**

**DEPARTMENT OF ELECTRONICS AND COMMUNICATION ENGINEERING**

**MALAVIYA NATIONAL INSTITUTE OF TECHNOLOGY, JAIPUR**


**2019**

**DEPARTMENT OF ELECTRONICS AND COMMUNICATION ENGINEERING**
**MALAVIYA NATIONAL INSTITUTE OF TECHNOLOGY**
**JAIPUR - 302017 , RAJASTHAN, INDIA**

## CERTIFICATE

This is to certify that the Dissertation Report entitled "**simulation based study of double gate tunnel field effect transistor as a biosensor**" by **Hemant chola** is the work completed under my supervision and guidance, hence approved for submission in partial fulfillment for the award of degree of Master of Technology in VLSI to the Department of Electronics and Communication Engineering, Malaviya National Institute of Technology, Jaipur in the academic session 2018-2019 for full time post-graduation program of 2017-2019.

**Date:**

**Place:**

**Dr. Tarun varma**
**Associate Professor**
**(Project Supervisor)**

**Department of Electronics and Communication Engineering**
**Malaviya National Institute of Technology, Jaipur**

---

# DECLARATION

I declare that,

a) The work contained in this dissertation is original and has been done by me under the guidance of my supervisor.

b) The work has not been submitted to any other institute for any degree or diploma.

c) I have followed the guidelines provided by the institute in preparing the dissertation.

d) I have conformed to the norms and guidelines given in the Ethical code of conduct of the institute.

**Date:** **Hemant chola**

**(2017PEV5093)**

# ACKNOWLEDGEMENT

I take this opportunity to express my deep sense of gratitude and respect towards my supervisor of the Dissertation, **Dr. Tarun varma,** Associate Professor, Department of Electronics & Communication Engineering, Malaviya National Institute of Technology. I am very much indebted to him for the generosity, expertise and guidance I have received from him while working on this project and throughout my studies. Without his support and timely guidance, the completion of my project would have seemed a far–fetched dream. In this respect, I find myself lucky to have him as my Project guide. He has guided me not only with the subject matter, but also taught me the proper style and techniques of working.

I would also like to thank **Prof. D. Boolchandani**, Professor of Electronics & Communication Engineering Department for his co-operation and help rendered in numerous ways for the successful completion of this work.

**Hemant chola**

**(2017PEV5093)**

# ABSTRACT

With the advancement in technology various devices are designed with the complex structure of processors. In this simulation the study of Double Gate Tunnel FET device parameters are studied to meet the requirements of the technological developments. The scaling of large devices is done to fabricate more no. of devices on a single structure. The integration of large devices into small chip provides efficient advantages with a smaller area. But as the number of devices increases the amount of supply voltage required is high as well as the decreases in the area increases the device OFF- state current.

To reduce all these problems TFET structure was designed to provide lower sub threshold swing. Several other structures like double gate tunnel FET is used to increase the ON-state current. The high- k and low-k dielectric were used with double gate. The high-k dielectric increases the channel capacitance and decreases the amount of sub threshold swing. Hence, the amount of supply voltage decreases and the power consumption is also reduced.

To enhance the tunneling in the device new modification in structure is introduced in which four regions are there P-N-P-N double gate structure. It has been observed that the amount of current increases in the presence of neutral as well as charged biomolecule because the tunneling width decreases and flow of carriers increases easily so, the effect was applied on double gate structure to get the desirable amount of current.

# CONTENT LIST

**DECLARATION……………………………………………………………………(i)**

**ACKNOWLEDGEMENT…………………………………………………………..(ii)**

**ABSTRACT………………………………………………………………………(iii)**

**CONTENT LIST ........................................................................................................(iv)**

**LIST OF FIGURES.........................................................................................................(vi)**

**Chapter 1 Introduction ...........................................................................................(1-10)**

1.1 MOSFET……………………………………………………………………1

1.2 Modes of operation……………………………………………………….....2

1.3 Limitation of mosfet…………………………………………………...............3

1.4 Sub threshold swing…………………………………………………………4

1.5 TUNNEL FET……………………………………………………………….....5

1.5.1– Introduction…………………………………………………………....5

1.5.2– structure and device operation…………………………………...........6

1.5.3– band to band tunneling………………………………………………......6

1.6 Double gate TFET structures………………………………………………......7

1.6.1 device structure and its operation……………………………………………7

1.7 Label free type of biosensor……………………………………………............8

1.8 Field effect biosensor…………………………………………………………......9

1.8.1 Types of ISFET based biosensor……………………………………........10

**Chapter 2 SIMULATION METHODOLOGY……………………………………(12-18)**

2.1 Introduction……………………………………………………………………......11

2.2 steps used for defining a structure…………………………………………………12

2.3 specification of models…………………………………………………………......14

2.4 common models…………………………………………………………........15

2.5 Tunneling models…………………………………………………………………16

2.6 Numerical methods…………………………………………………………….....17

2.7 Method to obtain solution………………………………………………………...17

2.8 Prediction of results…………………………………………………………....18

2.9 Models used in simulation of devices under study…………………………,18

**Chapter 3 DEVICE STRUCTURE AND TYPES OF BIOMOLECULE...(19-28)**

3.1 Introduction…………………………………………………………………19

3.2 Device operation and structure……………………………………….......20

3.3 Sensor and its classification……………………………………………....21

3.4 what is the need of biomolecule sensor and its types…..……………………23

3.5 Optimisation of device parameters……………………………………..23

3.6 Device specifications…………………………………………………...28

**Chapter 4 SIMULATION RESULTS AND DISCUSSIONS………………….(29-38)**

4.1 Introduction……………………………………………………………….29

4.2 simulated structure of PIN TFET……………………………………………29

4.2.1 Input Characteristics OF PIN TFET………….......................................30

4.3 simulated structure of PIN TFET…………………………………….....31

4.3.1 Input Characteristics OF PIN TFET……………………………….....31

4.4 Energy band diagram OF TFET……………………………………………...32

4.5 Detection of neutral biomolecule……………………………………………33

4.6 Detection of charged biomolecule…………………………………………...36

4.7 sensitivity calculation……………………………………………………...37

**Chapter 5 CONCLUSION AND FUTURE WORK……………………………….(39)**

**REFERENCES……………………………………………………………………..(40-42)**

# LIST OF FIGURES

Figure 1.1 Conventional MOSFET Structure……………………………………….2

Figure 1.2 ID versus $V_{GS}$ characteristics of MOSFET………………………………3

Figure 1.3 Extraction of subthreshold swing from $I_D$ versus $V_{GS}$…………………...4

Figure 1.4 Structure difference in MOSFET and TFET…………………………….5

Figure 1.5 structure of double gate TFET…………………………………………..8

Figure 2.1 Inputs and Outputs of active device simulator…………………………..12

Figure 3.1 Proposed device structure……………………………………………....20

Figure 3.2(a) band diagram along channel when $V_G<V_A$……………………….....23

Figure 3.2(b) band diagram along channel when $V_G>V_A$…………………………23

Figure 3.3 ID versus Vgs for PNPN n- MOSFET with comparison with conventional MOSFET……………………………………………………………………………..25

Figure 3.4 Subthreshold swing versus gate voltage $V_G – V_T$ for PNPN n-MOSFET..25

Figure 3.5 Subthreshold swing at ID = 1 nA/µm and VD = 1 V for different pocket widths……………………………………………………………………………...26

Figure 3.6 Doping required for just full depletion criterion and subthreshold swing at 1 nA/µm and 100 nA/µm (Doping × Width1.4 ≈ Constant)…………………….27

Figure 3.7 ION/IOFF ratio comparison for the PNPN and the conventional SOI n-MOSFET for the same IOFF = 1 nA/μm at LG = 100 nm. N-pocket width = 4 nm and NDMAX = $5 \times 10^{19}$ $cm^{-3}$ for different LG……………………………………27

Figure 4.1 Simulated structure of pin TFET on silvaco Atlas……………………..29

Figure 4.2 The Log ID versus Vgs characteristics of Pin TFET shows Ion current in the order of $10^{-11}$…………………………………………………………………...30

Figure 4.3 Simulated structure of PNPN TFET on silvaco Atlas…………………31

Figure 4.4 The Log ID versus Vgs characteristics of PNPN TFET shows Ion current in the order of $10^{-4}$…………………………………………………………………31

Figure 4.5 Energy band diagram of a device when it is off state…………………..32

Figure 4.6 Energy band diagram of a device when it is ON state…………………33

Figure 4.7 Log Id versus Gate voltage for different dielectric constant of biomolecule…..34

Figure 4.8 Threshold voltage versus dielectric constant variation…………………35

Figure 4.9 Log $I_D$ versus Vgs for charged biomolecule……………………………36

Figure 4.10 Sensitivity linear variation with dielectric constant of neutral biomolecule……………………………………………………………………..38

Figure 4.11 Sensitivity in parabolic pattern with respect to charged on biomolecule.38

# List of Tables

Table no.1 variation in parameter like threshold voltage due to neutral biomolecule dielectric constant……………………………………………………………………35

Table no.2 variation in parameters of TFET like threshold voltage, Ion current due charged biomolecule…………………………………………………………………37

# Chapter 1 Introduction

With the modernization in technology processors were designed with efficient usage. Since past few decades, the MOSFETs are scaled down to increase more functionality in device and design a structure with the integration of more transistors on a single device. Certain conditions were provided by ITRS, Firstly the advancement of scaling includes less power consumption with more no. of transistors on a single chip and simulation of three dimensional structure.

The second one includes the combination of heterogeneous technology and designing the new devices with the efficient way.

With the introduction of new technology, the power consumption has increased. The device which are best suited for low power consumption are CMOS with scaling of device on large scale. But the rate of increase in transistor is greater than the rate of increase in area due to scaling. As a result of which the temperature increases. This causes to increase in power dissipation of model. The static power consumption is calculated as leakage OFF state current multiplied by supply voltage and dynamic power consumption depends of frequency of operation and well as capacitance. So it is required to scale the value of supply voltage for proper functioning else the power consumption is high, which increases the heating effects in the device and causes the damage in the instrument. So to solve these problems faced by the conventional MOSFET research has been done to find other devices with less power consumption and reduced sub threshold swing.[1]

## 1.1 MOSFET

MOSFETs are developed gradually from the MOS integrated circuit technology. MOSFET is a four terminal device which can be applied in analog and digital circuits. An Insulated layer of dielectric material which is mainly $SiO_2$ is deposited over silicon substrate its structure is same as planar capacitance. There are four terminals gate, source, drain, and body in which body is connected to source hence making it four terminal device.

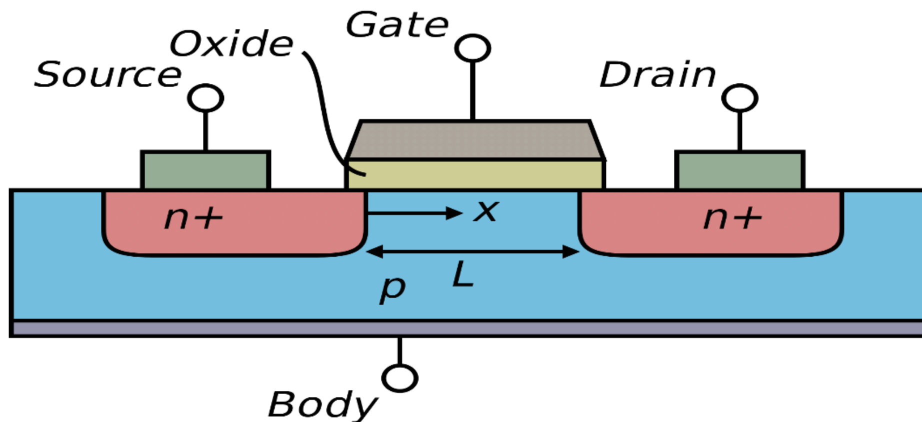


.

Figure 1.1 Conventional MOSFET structure

MOSFET structure: The current flow is supported by the electrons. Source and Drain regions are formed by using n+ regions. In enhancement mode, channel starts forming between source and drain. When sufficient positive voltage is applied between gate and source the holes are repelled which leads forming a channel with negative charges. As gate voltage further increased, electron density at the inversion layer increases and current flow from drain to source increases.

## 1.2 MODES OF OPERATION

There are three modes of operation of MOSFET:

1) cut off region: The Transistor is operated to be in off state and Drain current is zero. Applied gate voltage is less than the threshold voltage, which is not sufficient to form the channel.

2) linear or triode region: The applied gate voltage is increased such that it is greater than the threshold voltage, the current starts flowing between drain and source, drain to source voltage is less than difference of gate source voltage and threshold voltage.

3) Saturation region: For saturation region gate to source voltage is greater than the threshold voltage, as well as drain to source voltage is greater than difference of gate to source voltage and threshold voltage, in this region the MOSFET behaves as an ideal current source.

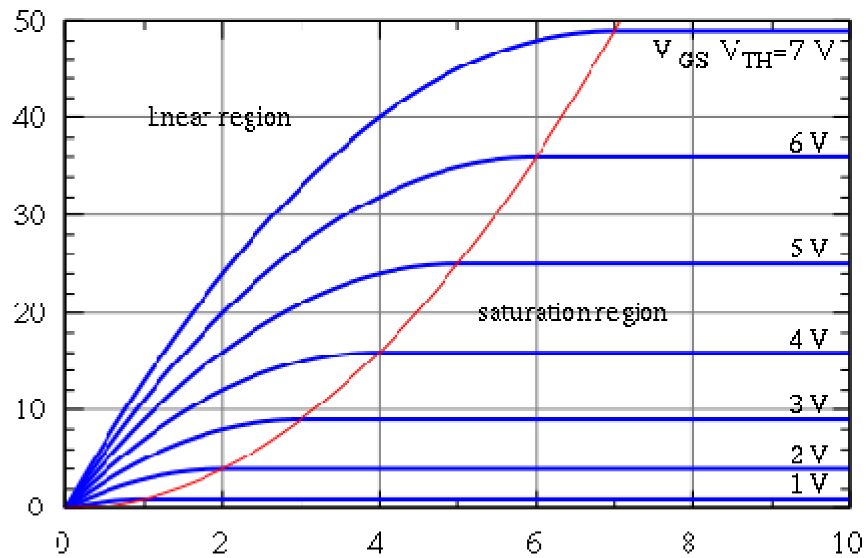


Figure 1.2 $I_D$ versus $V_{GS}$ characteristics of MOSFET

## 1.3 LIMITATIONS OF MOSFET

1) leakage current- when Vgs<$V_t$ ,the drain current supposed to be zero but the current decreases exponentially. To measure this leakage current we take the help of sub threshold swing which is given by the amount of gate voltage applied to produce 10 times the change in current.

Its value is constant to 60 mv/decade for leakage current to zero at room temperature. When scaling is done on the device to reduce power dissipation the sub threshold swing should be around 60 mv/decade.

2) Short channel effects

a) Velocity saturation effect – Due to the scaling of MOSFETs to lower dimensions very high electric field is experienced by the charge carriers. Due to high electric field the velocity of carrier starts saturated which degrade the performance.

b) Drain Induced Barrier Lowering – In long channel devices, the threshold voltage is independent of drain voltage but in short channel device the drain voltage start influence the channel carrier which start flowing current at gate voltage less that threshold voltage.

c) Impact Ionization- Due to high electric field the velocity of electrons is very high. They impact on silicon atoms which break the bond and create new electron and hole pair. This is called impact ionization.

d) hot carrier effect- Due to this, the electrons and holes enter into dielectric after gaining high kinetic energy. This changes the capacitance of the system and makes it less reliable.

## 1.4 SUBTHRESHOLD SWING

It is the amount of gate voltage required to provide a one decade change in current. Sub threshold swing for a Tunnel FETs changes with the change in gate voltage, it varies not constant. At low gate voltages, for Tunnel FETs, it is possible to have this value less than 60 mV/decade compared to MOSFET at room temperature. Tunneling current from a p-n Junction with reverse biased.

It is cleared from the above sub threshold swing value that it is dependent on $V_{GS}$. As gate voltage decreases, the subthreshold swing value decreases and it increases with the increase in gate voltage. Therefore, the value of subthreshold swing is not linear with the $I_D$ and $V_{GS}$ curve and may have different values.

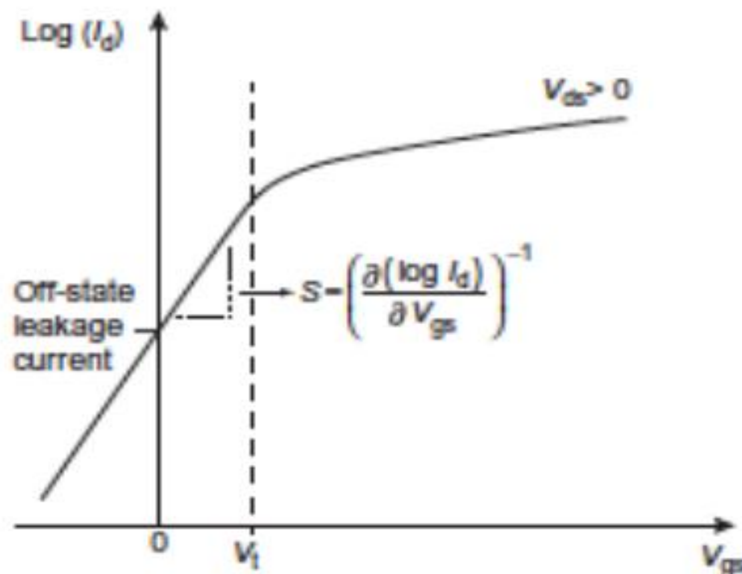


Figure 1.3 Extraction of subthreshold swing from $I_D$ versus $V_{GS}$

## 1.5 TUNNEL FIELD EFFECT TRANSISTOR

The Tunnel FET has the same structure as MOSFET but differs in the switching techniques and switching can be done at low voltage than MOSFETs. This device is more useful in low power applications due to its low sub threshold swing and low OFF-state current. Unlike conventional MOSFETs the shorts channel effects are removed in Tunnel FETs because the current is controlled by a tunneling phenomenon. It works on the principle of the band to band tunneling which makes it operate at the low sub threshold swing. Tunnel FET is a gated p-i-n diode which works on the basis of reverse bias. Source and drain region are heavily doped with p+ and n+ regions.

### 1.5.1 TFET STRUCTURE AND ITS OPERATION

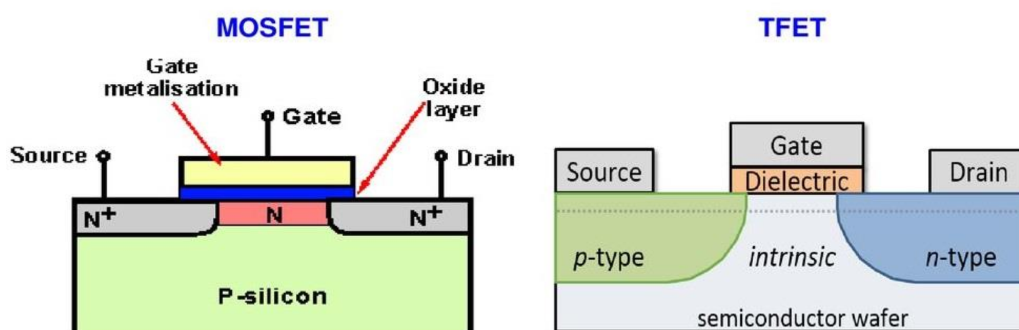


Figure 1.4 structure difference in MOSFET and TFET

Tunnel FET is a gated p-i-n diode. Due to its heavily doped p+ and n+ region, depletion region forms at the junction of intrinsic region and the n+ doped drain region. When a reverse bias has applied the width of the depletion region starts increasing, producing the swept charge carriers. These charge carriers tunnel through intrinsic region to source valence band by the band to band tunneling phenomenon.

TFET can be of two types n- type in which source is p+ doped and drain is n+ doped and a positive voltage is applied to the gate terminal. And other is p-type in which source n+ doped and drain is p+ doped and negative voltage is applied to gate.

### 1.5.2 BAND TO BAND TUNNELING

It is a phenomenon of conduction of current used in Tunnel Field Effect Transistor. The phenomenon of tunneling is same in a Tunnel diode. The Fermi level present in the conduction band of n-type drain and valence band of the p-type source region. The electrons are present in n- type drain and holes are present in p- type source. At zero bias condition due to heavily doped p+ and n+ region, the conduction band of n side and the valence band of p side becomes align to each other . When applied reverse bias increases the height of potential barrier decreases and electric field increases. This causes the electrons from the conduction band of n- type drain flow to the valence band of p- type source side, due to which the current increases and max current flows.

Tunneling is of two types direct and indirect. In direct tunneling, the electrons pass from the valence band to conduction band without any absorption or emission of photons. The examples of this tunneling are GaAs etc. In indirect tunneling, there is a change of momentum due to absorption or emission phenomenon when the electrons are transferred from valence band to conduction band. The examples of the indirect band to band tunneling are germanium, silicon etc.

### 1.5.3 ADVANTAGE AND DISADVANTGE

ADVANTAGES

TFET has feature that makes it efficient transistor in the upcoming future. The current carrying transport mechanism in the devices is different from MOSFET. As MOSFET uses drift and diffusion method for transfer of carriers and TFET uses the band to band tunneling process. MOSFET performance effects by the temperature is high as compared to tunnel FETs which are less dependent on temperature. Therefore, TFETs has sub threshold potential is less than or equal to 60 mv/decade. In TFETs the tunneling width is controlled by the gate voltage and leakage current is less.

The value of sub threshold swing is reduced which reduces the amount of supply voltage required to operate and hence static and dynamic power dissipation is less. This decreased value of sub threshold swing helps them to behave as an ideal switch with the change in gate voltage in a small amount.

DISADVANTAGE

In silicon Tunnel FET the ON current is less since band to band tunneling is not much effective which is needed to be overcome.

The scaling on high scale of the device leads to very high OFF current and can vary the transistor performance.

The current flows for both the polarity of gate voltage gives ambipolar nature of TFET. It shows p -type behavior with excess holes and n -type with excess electrons. TFETs show the dominant phenomenon of ambipolar nature, in which symmetric structures and the level of doping of drain and source is done same with single material of gate dielectric.

## 1.6 DOUBLE GATE TFET STRUCTURE

Double gate Tunnel FET consist of conducting channel surrounded by the gate electrodes on both sides and the channel is formed in between. Double gate tunnel FET plays a very important role in decreasing the OFF current by providing better control over the channel.

### 1.6.1 DEVICE STRUCTURE AND OPERATION

In this work, the study of TFET with single and double gate, using different gate dielectrics and using dual material gate is done to improve the current and to achieve efficient characteristics. The simple model of the double gate is studied to get the desired amount of current with suitable sub threshold voltage. There is always the benefit of the extra gate like extra current can add to the original one. Hence, ON current is increased. The presence of two gate forms two tunneling junctions hence there is an increase in current and the OFF current is same in the range of pa. Sub threshold swing is decreased and $I_{on}/I_{off}$ ratio is increased making it the suitable device for operation.[2]

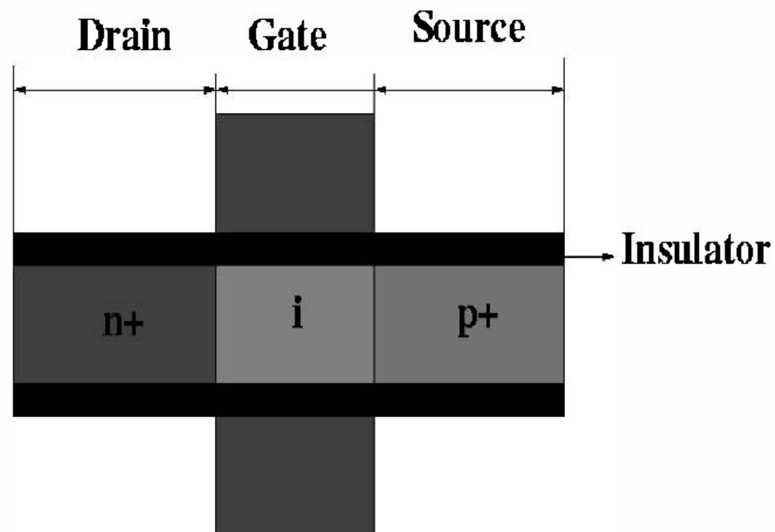


Figure 1.5 structure of double gate TFET

The working principle is same as tunnel FET and follows the band to band tunneling for the conduction of current. Voltage is applied to the gate terminal which controls the electric field and it provides the better control over channel current. The presence of double gate improves the control over tunnel junction with the gate voltage and this causes the current to increase by double amount coming from the thin device body. hence, the sub threshold swing is decreased.

The doping level plays an significant role to enhance the device characteristics like an increase in ON current and decrease in OFF current. The doping in source region should be high for the optimized on current and desirable characteristics because of the tunneling between the source and intrinsic region. The OFF state current depends on the doping level in the drain region. The ambipolar behavior of the transistor is shown when the doping levels are equal in both source and drain region. The undesirable characteristics can be reduced by decreasing the doping level in drain side. This also decreases the OFF current level. The gate threshold voltage differentiates or checks the changes in the tunnel junction width through the energy barrier.

## 1.7 LABEL FREE TYPE OF BIOSENSOR

A biosensor is an analytical device converting a biological information into a quantifiable and process able signal. Since the research by Clark and Lyons in 1962 on the first biosensor. The demand on such analytical tools in diagnostic applications was increasing. With the

growing number of deaths due to late diagnosis and the high number of diseases being diagnosed in the world, biosensors are a critical tool in the early disease diagnosis.

In clinical laboratories, as described above, ELISA is the most common biomarkers detection method. It can detect more than hundred types of diseases. In biomarkers detection, most of the techniques currently employed use various labels or reagents like enzymatic, fluorescent or radiochemical labels. The labelling processes may hinder monitoring of the probe/target interaction rapidly. In other words, the labeling may affect the target-receptor interactions, which are caused by steric hindrance, induced by the label. In spite of the low detection limits and high sensitivity, these methods are still expensive, complex and time-consuming. Additionally, such methods often require laboratory personnel with high skills. Thus, the development of sensitive, simple and high-throughput biosensors that are able to detect biomarkers without involving labeling is of great interest. Label-free bio sensing would eliminate the process steps for the modification and preparation of the target molecules, which significantly save the costs and time needed for sample preparation. Label-free biosensors are potentially very useful as clinical diagnostic tool, thanks to real-time and multi-analyte tests, quick detection and inexpensiveness.

So far, electrochemical transducers are being extensively used in biosensor. Among the variety of electrochemical transducers proposed for detecting biomolecules without labeling, the field effect transistor (FET) is an attractive approach. The FET biosensor can analyze kinds of biomarkers such as DNA and proteins without labeling and in a rapid, simple and inexpensive way.

## 1.8 FIELD EFFECT TRANSISTOR (FET) BASED BIOSENSOR

Many types of biosensor exist in the fields of biomarker detection. FETs have been also used for the label-free detection of bio recognition events, such as antibody-antigen reactions, glycan-protein interactions, DNA hybridization reactions and cell identification.

The FET biosensors are sensitive to the intrinsic electric charge of biomolecules. By modification of the FET gate surface with a bio molecular layer as a receptor, the changes in the gate voltage-drain current caused by the adsorption of analyte biomolecules can be detected. Since target molecules are charged in an aqueous solutions, the charge on the gate surface changes with bio recognition, and its density variation is transduced by field effect into an electrical signal. The bio recognition events on the FET gate surface can be found by detecting a shift of the threshold voltage. The immobilization of various bio recognition

materials on the FET gate surface for biomarker analysis has been developed through surface modification technology.

Among many different types of FET devices, (MOSFET, MESFET, JFET and CHEMFET among others), commonly bio sensing applications are focused on ISFET (ion-selective field-effect transistor) devices. ISFET was firstly described by Bergveld in 1970, which was used as a transducer in electrochemical sensors for electrophysiological measurement of ion composition around nerve tissues. Several types of ISFET-based biosensors exist. Some forms of ISFET-based biosensors, such as enzyme ISFET, immuno ISFET, DNA-based ISFET and cell-based ISFET are explained in detail in this section.

### 1.8.1 TYPES OF ISFET BASED BIOSENSOR

1. Enzyme based ISFET : The concept of Enzyme ISFET revolves around the principle of pH-sensitive ISFET, stating that the enzymes are immobilized on the gate surface of the ISFET device. So far, enzyme ISFET is applied on the detection of numerous analytes such as penicillin, urea, glucose, pesticides etc. it was proven that the enzyme ISFET might be suitable for quick and sensitive detection of small amount of analytes, with the advantage of saving analysis time. Thus, this ISFET enzyme biosensor has been found to have potential of detection of complex samples.

2. DNA based ISFET: DNA molecules are negatively charged in an aqueous solution. The amount of negative charge at the gate surface increases when DNA strands bind to the ISFET gate surface. The FET could transduce the variation of charge density into an electrical signal, thereby allowing for excellent performance of DNA analysis.

3. CELL based ISFET: Cells' activity during their life can be monitored, and these data have applications in biomedicine and pharmacology. Cell-based ISFET has been considered as a promising tool for providing a variety of biologically active information of living cells Cells activity during their life can be monitored, and these data have applications in biomedicine and pharmacology. Cell-based ISFET has been considered as a promising tool for providing a variety of biologically active information of living cells.

But the problem with ISFET is that it can only used for charged biomolecule not for neutral biomolecule. Therefore dielectric modulated n type PNPN TFET is introduced.

CHAPTER -2 SIMULATION METHODOLGY

## 2.1 INTRODUCTION

Atlas is a software provides general potentials for physically-based two and three dimensional (2D, 3D) simulation of semiconductor devices. Atlas is designed in such a way that it can be used with the VWF Interactive Tools. The VWF (Virtual Wafer Fabrication) interactive Tools consist of the following: Mask Views, Optimizer, Deck Build, Tony Plot, and dev edit. Their functions are explained below:

1. Deck Build puts forward the condition for running Atlas command language.
2. Optimization across various simulators can be provided by Optimizer.
3. Through Tony Plot the outputs which are actually the electrical characteristics of the device along with structure files generated for the designed device can be seen.
4. IC layout correction is done by Mask Views.

Along with Atlas, there exists another process simulator called Athena. It can produce structure by many processing steps. The same structures can be used by Atlas as inputs. Later Atlas predicts the electrical characteristics related to the designed device. Now the outputs of the Atlas can be given as the used as the inputs to the SPICE modeling software and Utmost device characterization.

Atlas can be called as a physically-based simulator for devices as it is capable of calculating all the characteristics of a particular device with specified structure and voltage biases at the electrodes. The device area is divided by these simulators with grids called meshes and with mesh points called nodes. By applying differential equations which are derived from Maxwell laws, current conduction and electrical parameters a teach location through the structure is determined. This type of physically based simulation has many advantages like, they provide a deep insight of the attributes of advice without experimentally creating the device, calculation of very complex parameters are done very easily and quickly, estimation of the trends with the varying properties of the device according to its different bias conditions can be estimated through these simulations.[3]

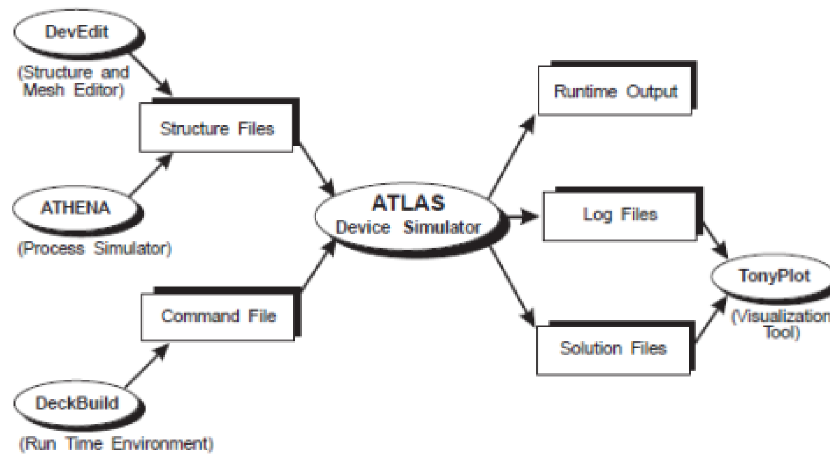


Figure no.2.1 Inputs and Outputs of active device simulator

Information flowing through Atlas device simulator can be seen in the above diagram (Figure2.1). The text file, which contains Atlas command language and structure file, which has the structure on which simulations has to be performed are the two input files to Atlas device simulator. Atlas gives three types of output files: runtime output which gives the information being processed at every instant of execution of Atlas commands and simultaneously show the errors and warnings. log files which gives all the electrical characteristics which is specified in the Atlas command language and solution files which has the 2D or 3D data of the device parameters at each and every point in the device.[3]

## 2.2 STEPS TO DEFINE SIMULATED STRUCTURE:

There is sequence of step we have to follow to write code in silvaco atlas simulator:

**STEP 1** Define meshing : Mesh specification starts with a mesh mult statement which multiplies the spacing between the meshes by a factor (taken along with mesh. mult command) so that finer or coarser meshes can be created according to the need.

Syntax:

```
Mesh space.mult=<value>
Eg: Mesh space.mult=4.0
```

After this x.mesh and y.mesh statements are specified as follows:

```
X.mesh LOC=<value1>SPAC =<value2>
```

```
Eg: X.mesh loc=0.00 spac=0.0001
Y.MESH LOC=<value3>SPAC=<value4>
Eg: Y.mesh loc=0.00 spac=0.0001
```

where `value1` and `value3` specifies the location of vertical and horizontal mesh line in microns respectively and `value2` and `value4` specifies the spacing between these mesh lines.

**STEP 2** Define regions: Different regions consist of different materials with a specific doping profile. For specifying the region the following command is used:

```
REGION
NUMBER=<value>X.MIN=<value1>X.MAX=<value2>Y.MIN<value3>Y.MAX
=<value4>MATERIAL=<material1>
Eg: Region number=1 x.min=-0.010 x.max=0.00 y.min=0.00
y.max=0.010 material=Silicon
```

The region number is specified by `value` and „`value1` to `value2` gives the range of the region on the x-axis while `value3` to `value4` on y-axis. `material1` is the material forming the region (like Silicon, $SiO_2$ etc).

**STEP 3** Define electrodes :

```
ELECTRODE
NAME<electrode1>NUMBER=<value>X.MIN=<value1>X.MAX=<value2>Y.
MIN<value3>Y.MAX=<value4>
```

Where the name of the electrode is given as „`electrode1`‟. The location of the electrode is from x.min to x.max and y.min to y.max.

**STEP 4** Define doping:

```
DOPING<doping profile>CONC =<value><dopingtype>REGION=<number>
Eg: doping uniform conc=1e14 n.type direction=y region=2
```

Doping profile can vary with its concentration and type of doping which are specified by *value* and *doping type* respectively. The doping profile can be either be uniform or Gaussian.

**STEP 5** Contact name: following syntax is required:

```
CONTACT NAME<contact name>WORKFUNCTION=<value>
Eg: contact name=source neutral
```

where name of the contact is given by *contact name* whereas its work function is specified by *value*

Instead of specifying the work function by *value*, it can also be specified by their name in the contact statement for the commonly used contacts like N.Polysilicon, P.Polysilicon, Aluminium, Tungsten, etc. The statements used for this type of contacts are:

```
CONTACT NAME<f.gate> N.Polysilicon.
```

## 2.3 SPECIFICATION OF MODELS:

Usually the statements for MODELS are used to indicate the physical models which are required for simulations. The selection of the MODELS is according to the physical phenomenon occurring inside the considered device. These MODELS be divided into the following 5 categories

1. Carrier Statistics Models
2. Mobility Models
3. Recombination Models
4. Impact Ionization Models
5. Tunneling and Carrier Injection Models.

## 2.4 COMMON MODELS:

1. Concentration-Dependent Low-Field Mobility Model: To activate this model, CONMOB is used in the MODELS statement. This model provides the data for mobilities of electrons and holes at low field for silicon and gallium arsenide only at 300K.

2. Analytic Low Field Mobility Model: To activate this model, ANALYTIC is used in the MODELS statement. This model helps in specifying temperature and doping dependent low field mobilities. This model is also specified by default for silicon at 300K.

3. Lombardi CVT Model: CVT in the models statement are used for activating this model. This models priority is much more than all other mobility models. In this model, Matthiessen's rule is used for combining the components associated with mobility dependent on transverse field, temperature and doping. On activating this model by default, Parallel Electric Field Mobility Model will also get activated.

4. Shockley-Read-Hall Recombination Model: The SRH parameter is used in the MODELS statement for activating this model. There are a few user-definable parameters that used in the MATERIAL statement, like TAUN0 and TAUP0 the electron and hole lifetime parameters. This model gives the recombination of electron and hole through Shockley-Read-Hall recombination method happening within the device.[3]

5. Boltzmann Model: This model is the default carrier statistics model. It is activated by specifying BOLTZMANN in the MODELS statement. As the name indicates this model follows Boltzmann statistics.

6. Fermi-Dirac Model: This model follows Fermi-Dirac statistics. It is usually in those regions which are heavily doped but with reduced concentrations of carrier. To activate this model FERMI is used in the MODELS statement.

## 2.5 TUNNELING MODELS:

1. Standard Band To Band Tunneling Model: For high electric field, present in the considered device, tunneling of electrons can be caused by the localized electric field such that there is a bending of energy bands at the junction of tunneling. For such kind of application standard band to band tunneling model can be used. This model can be used BBT.STD needs to specified in the MODELS statement. The tunneling rate can be calculated by the following equation:

$G_{BBT} = D \times BB.A \times e^{BB.GAMMA} \times e^{(-BB.B/E)}$

Where *D* is the statistical factor, *E is* electric field. BB.A, BB.B, and BB.GAMMA are user definable parameters with default values

BB.A = 9.6615e18 $cm^{-1}\ V^{-2}\ S^{-1}$

BB.B= 3.0 e7 V/cm

BB.GAMMA= 2.0

2. Non-local Band-to-Band Tunneling Model: This model is nonlocal in nature unlike all the rest of the models. The spatial variation of energy bands are taken into consideration by this model. It also considers the fact that generation recombination rate at each point does not depends only on the electric field local to the point. According to BBT.NONLOCAL the tunneling happens through 1D slices, at the tunnel junction where each slice and the tunnel junction are perpendicular to each other. These slices are para to themselves. The tunnel slices specification can be done in two different ways. They are:

(i) Making rectangular area around the tunnel junction using the statements QTX.MESH and QTY.MESH.

(ii) Making a region surrounding the tunnel junction using statements QTREGION

The first method is applicable for only planar junctions while second method can be used for both planar and non-planar junctions.

## 2.6 <u>NUMERICAL METHODS:</u>

The numerical methods are specified in the METHODS statement. To find solution there are three different types of techniques:

1. Gummel
2. Newton
3. Block

The first method finds solution for one unknown variable while the rest of the variables are constant. This process will continue until a stable solution is obtained. Unlike the gummel method, newton method solves and finds all the unknowns at the same time. Block method is in between newton and gummel methods as it solves a few unknowns at the same time gummel is generally used for the device studied in this project i.e. the tunnel FET.

## 2.7 <u>Methods to obtain solutions:</u>

To calculate current as well as other parameters such as carrier concentrations and electric fields, the device electrodes needs to be supplied with voltages. At first, electrodes are provided with zero voltages, after that the bias voltage applied is varied in small steps. These needs to be specified in the SOLVE statements.

1. <u>DC Solution</u>: A fixed DC bias can be applied on the electrode by using the DC solve statements. SOLVE <v.*electrode name*>=<*value*>.

According to this statement the required electrode, *electrode name* is supplied with DC voltage *value*.

For sweeping the bias of a particular electrode from *value1* to *value2* in a particular order of steps *step1*, the following command is used.

```
SOLVE <v.electrode name>=<value1> VSTEP=<step1> VFINAL=<step2>
NAME=<electrode name>.
```

Convergence can be obtained for the used equations by supplying a good original presumption for the variables that need to be evaluated at each bias point. Initial solution can be achieved by the given statement, SOLVE INIT.

2<u>. AC Solution: </u>A simple extension of the DC solution syntax can specify the AC simulations. A post-processing operation to a DC solution leads AC small signal analysis.

The conductance and capacitance between each pair of electrodes is the results of AC simulations. The command used for this is

SOLVE $V_{BASE}$=0.7 AC $F_{REQ}$=1e9 $F_{STEP}$=1e9 $NF_{STEPS}$=10

## 2.8: Prediction of results:

The output files of Atlas are of three different types. They are:

1. Run-Time Output: The output seen at the bottom of the Deck Build Window is the run-time output. Any errors occurring during this output will be displayed in the run-time window.

2. Log Files: These files are required for storing the terminal characteristics calculated by Atlas. It consist of the current and voltages for each electrode during the DC simulations. In transient simulations, the time is saved. Whereas for AC simulations, the conductance, capacitances and the small signal frequency are stored.

3. Extraction of parameters In Deck Build: For this the EXTRACT command is introduced inside the Deck Build environment. Thus extracting the various parameters of the device. The command has a flexible syntax that allows you to construct specific EXTRACT routines. EXTRACT can operate on the earlier solved curve or structure file.

## 2.9 Models used in simulation of devices under study:

As Double GATE TFET is the studied topic of this thesis, nonlocal band-to-band tunneling model has been considered for the simulation purpose. Apart from nonlocal BTBT model, the other models were also taken into consideration like recombination models like srh models, concentration field mobility model. The carrier statistics model used for this simulation is Fermi model.

# CHAPTER -3 DEVICE STRUCTURE AND ITS OPERATION

## 3.1 INTRODUCTION

MOSFET scaling gives rise to a number of critical issues such as source/drain-to channel electrostatic coupling, channel transport limitations, gate tunneling and parasitic effects. Due to short-channel effects (SCEs) such as drain-induced barrier lowering (DIBL), deeply scaled mosfets typically have greater than the 60-mV/dec diffusion limited subthreshold characteristics at room temperature. Together with constraints on supply voltage scaling, high IOFF and reduced ION/IOFF ratio are thus expected for sub-65nm conventional MOSFETs. Moreover, with shrinking dimensions, power dissipation is becoming a major concern. As a result reduction in IOFF is necessary for low leakage currents and to minimize standby power. To overcome these problems, novel engineering solutions such as improving the device architecture.

As an alternative solution toward achieving steep subthreshold swing transistors, we propose a novel device concept of the tunnel source (PNPN) n-MOSFET. Its operation and optimization will be examined. Fig.3.1 shows the device structure of the novel asymmetric PNPN n-MOSFET. Instead of an n+ source as in a conventional MOSFET, a tunneling junction formed between a p+ region and a narrow fully depleted n+ layer under the gate acts as a source of electrons for the channel. The thin fully depleted n+ layer reduces the tunneling width and increases the lateral electric field, thereby minimizing subthreshold swing as well as potential drop at the tunneling junction.

Thereafter, the concept of dielectric modulated FET (DMFET) was proposed, with nanogap cavity at both source and drain ends enabling the label-free detection of neutral biomolecules as well with high sensitivity. A reported DMFET for the label-free DNA detection technique taking into consideration both the dielectric constant and the charge possessed by a biomolecule.

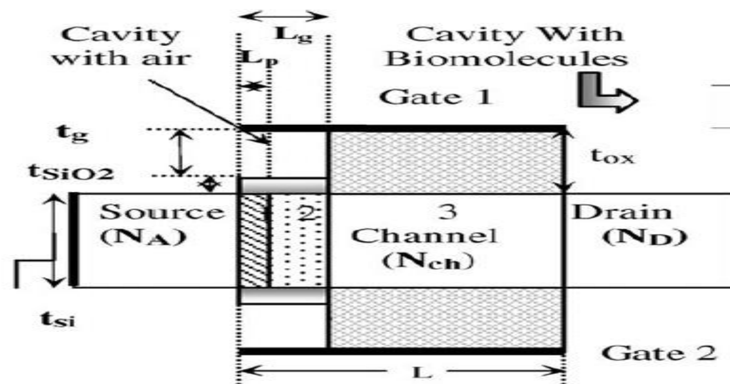


Figure .3.1 Proposed device structure

**REFERENCE**: Rakhi Narang ,K. V. Sasidhar Reddy , Manoj Saxena , R. S. Gupta , Mridula Gupta "A Dielectric-Modulated Tunnel-FET-Based Biosensor for Label-Free Detection"IEEE ELECTRONIC DEVICE LETTERS VOL.33.no.2 feb 2012

## 3.2 WHAT IS SENSOR?

A sensor is a device that responds to input from the physical environment. The specific input could be light, heat, motion, pressure, or any one of other environmental phenomena.

Generally the output signal is converted to readable display at the sensor location or transmitted electronically over a network for further processing.

## CLASSIFICATION OF SENSOR

### FIRST CLASSIFICATION OF THE SENSOR:

Active Sensors :They are those which require an external excitation signal or a power signal. Eg : temperature sensors, alcohol sensor, gyro sensor etc

Passive Sensors : They do not require any external power signal and directly generates output response. Eg : infrared camera or PIR sensor uses external heat energy to capture images.

### SECOND CLASSIFICATION OF THE SENSOR:

It is based on the means of detection used in the sensor. Some of the means of detection are Electric, Biological, Chemical, Radioactive, ph sensor etc.

**THIRD CLASSIFICATION OF THE SENSOR :**

It is based on conversion phenomenon i.e. the input and the output. Some of the common conversion phenomena are Photoelectric, Thermoelectric, Electrochemical, Electromagnetic, Thermo optic, etc.

**THE FINAL CLASSIFICATION OF THE SENSOR :**

These are Analog and Digital Sensors. Analog Sensors produce an analog output which is a continuous output signal with respect to the quantity being measured. Digital Sensors, work with discrete or digital data. The data in digital sensors is digital in nature.

## DIFFERENT TYPES OF SENSOR IN ELECTRONICS

These sensors are used for measuring one of the physical properties like Heat Transfer, Temperature, Resistance, Conduction, Capacitance, etc. are oftenly used in most of the electronics applications.

1. Temperature Sensor
2. Accelerometer
3. Proximity Sensor
4. Pressure Sensor
5. Ultrasonic Sensor
6. Touch Sensor
7. IR Sensor (Infrared Sensor)
8. Light Sensor
9. Smoke, Gas and Alcohol Sensor

## 3.3 WHAT IS NEED OF BIOMOLECULE SENSOR AND ITS TYPES:

Generally term used for biomolecule are molecule and ions that are present in organisms, typically in biological process such as cell division, development of cell.

Biosensors produce a digital electronic signal which is proportional to the concentration of a specific analyte or group of analytes. While the signal may be continuous or discrete, devices can be configured to measure in specific format. Examples of Biosensors include immuno sensors, enzyme biosensors, organism and cell-based biosensors.

These sensors are applied to variety of analytical scenario including medicine industry, biomedical research, drug discovery, the environment, food preservatives, process industries, security and defence.

## TYPES OF BIOMOLECULE:

There are 4 main groups of biomolecules (organic) :

1. Carbohydrates (made of Monosaccharides): Used for energy e.g glucose Can be structural as in plant cells (cellulose Builds cell walls)
2. Lipids/fats : Very important as they are made up of the phospholipid Bi-layer or all animal cells .This membrane regulates what can come in and what is needed by the cell
3. Proteins (made of Amino Acids) : It can be functional and structural structural proteins allow us to build muscle filaments etc. Functional enzymes include which allow almost all chemical reactions to occur faster rate and at less energy.

## THERE IS ANOTHER CATEGORY OF BIOMOLECULE:

1. Neutral biomolecule(k>1) : biotin, streptavidin, protein, APTES
2. Charged biomolecule: These are inorganic ions in the cell, including sodium ($Na^+$), potassium ($K^+$), magnesium ($Mg^{2+}$), calcium ($Ca^{2+}$), chloride ($Cl^-$), phosphate ($HPO_4^{2-}$). These ions are helps to enhance cell metabolism, and thus play critical roles in cell function.

## 3.4 DEVICE OPERATION

The operation of the tunnel source (PNPN) n-MOSFET based on the principle of band-to-band tunneling. It is important to point out that tunneling is prohibited not only by large tunneling barrier width but also by the Fermi selection rule (the availability of density of states to tunnel to). We define a voltage $V_A$ as the gate voltage required to align the p+ valence band to the channel conduction band. When $V_G$ is small ($< V_A$), the channel conduction band is above the p+ source and therefore, the current level is negligible since the electron from the p+ valence band can tunnel only to the trap state Fig.3.2(a)[4]

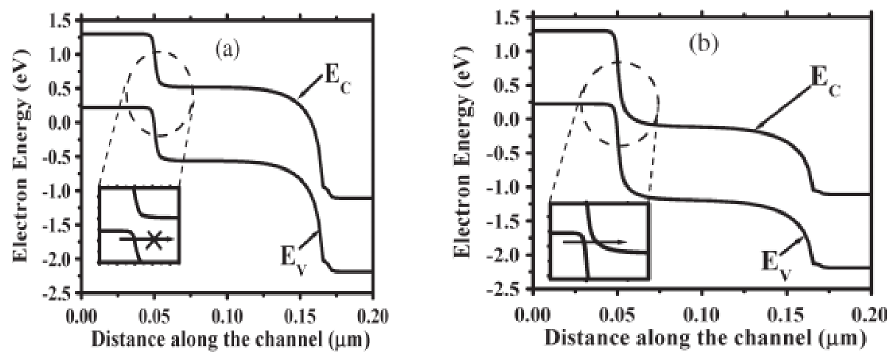


Figure 3.2(a) band diagram along channel when $V_G<V_A$. 3.2(b) band diagram along channel when $V_G>V_A$

As $V_G$ increases above $V_A$, tunneling width reduces and the channel conduction band goes below the p+ source= valence band. Consequently, there are states in the channel region for the electrons from the p+ source valence band to tunnel to Fig3.2(b) thus giving rise to the device current. As $V_G$ becomes high ( $V_A$), the tunneling resistance at the source junction decreases due to reduction in tunneling width and large density of available states for the electrons to tunnel into. Therefore, under large gate bias, device current is limited by the drift field in the channel as in a conventional MOSFET[4]

## 3.5 OPTIMISATION OF DEVICE PARAMETERS

Extensive device simulations were performed using SILVACO's device simulator ATLAS coupled with analytical tunneling calculations. Since the mechanism for indirect tunneling in Si and Ge can be described by empirical expressions, the calculations in our case were

based on the well known equations for the tunneling current $I_t$ of the Esaki tunnel diode shown as follows

$$I_t = I_{c\text{-}v} - I_{v\text{-}c} = A\int_{EC}^{EV} Fc(E) - Fv(E) \times T_t(E)\, n_c(E)\, n_v(E)\, D_e$$

$I_{C\rightarrow V}$ is the tunneling current from the conduction band to the empty state of the valence band and $I_{V\rightarrow C}$ is the tunneling current from the valence band to an empty state of the conduction band. *A* is a constant, $F_C(E)$ and $F_V(E)$ are the Fermi–Dirac distribution functions, and $n_c(E)$ and $n_v(E)$ are the density of states in the conduction band and valence band, respectively. In our calculations, the tunneling probability was defined as

$T_t = \exp(-C/E_{eff})$ ; $E_{eff} = E_g/W_{tun}$ where $C = \pi^2\sqrt{m}\, E_g^{3/2}/\sqrt{2}qh$

In which, m is the effective mass of the electron, $E_g$ is the band gap of silicon, q is the electronic charge, and h is the Planck's constant. $W_{tun}$ is the tunneling distance for each overlapping energy state. Parameters A and m were tuned to obtain a fit with the experimental data from silicon tunnel diodes.[4]

In which, m is the effective mass of the electron, $E_g$ is the band gap of silicon, q is the electronic charge, and h is the Planck's constant. $W_{tun}$ is the tunneling distance for each overlapping energy state. The tunneling formalism can therefore be used satisfactorily to simulate similar tunneling structures like the proposed tunnel source (PNPN) n-MOSFET. Although the simulation issues involving the tunneling mass, the effective tunneling distance and indirect. The doping profiles used for the simulation are boxlike and abrupt.[4]

### 3.5.1 Performance:

Fig.3.3 shows the comparison between the I–V characteristics for a PNPN n-MOSFET and corresponding conventional silicon-on-insulator (SOI) n-MOSFET with the same structural parameters (at the same $I_{OFF} = 10$ pA/$\mu$m). The n+-pocket is just fully depleted which is an important requirement for proper device operation. It is evident that with a narrow ( ∼4 nm) n+ region, the PNPN n-MOSFET shows a minimum subthreshold slope much less than 60 mV/dec at room temperature with negligible DIBL. In addition, it exhibits a higher drive current as compared to the conventional MOSFET. This is because for the same $I_{OFF}$, the PNPN nMOSFET has a lower $V_T$ on account of steeper subthreshold slope. At a given $V_G$, the PNPN device has a higher effective $V_G$-$V_T$ than the SOI case, leading to higher $I_{ON}$.

Thus, the PNPN n-MOSFET has the potential to meet low standby power and low operating power requirements. The tunneling-limited subthreshold swing is a function of $V_G$.[4]

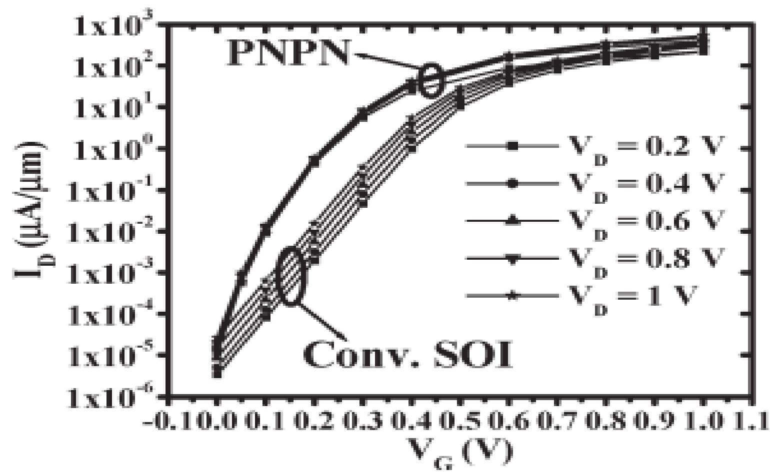


Figure 3.3 $I_D$ versus Vgs for PNPN n- MOSFET with comparison with conventional MOSFET

### 3.5.2 Optimisation of $n^+$ pocket:

Fig.3.4 shows the subthreshold swing (SS) versus $V_G$-$V_T$ for two pocket widths (4 and 15 nm) of the PNPN device compared with conventional SOI over a $V_G$-$V_T$ range of 0.55 V. The n-pocket doping is fixed at $5 \times 10^{19}$ $cm^{-3}$. For a width of 4 nm, the pocket is just fully depleted, and the subthreshold conduction mechanism is gate controlled band-to-band tunneling at the source.[4]

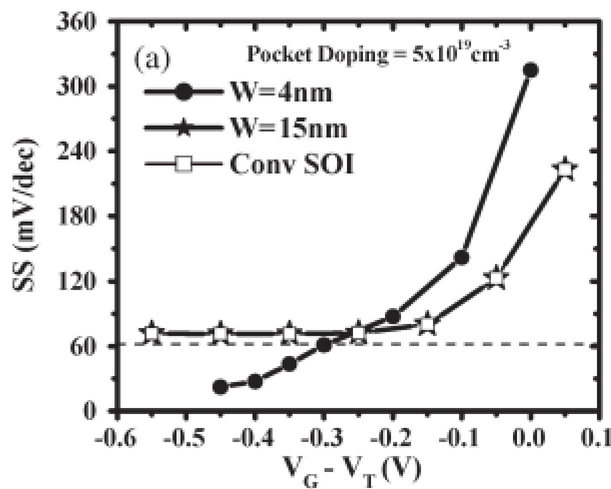


Figure 3.4 subthreshold swing versus gate voltage $V_G$ –$V_T$ for PNPN n-MOSFET

For a width of 4 nm, the pocket is just fully depleted. With further reduction in the pocket width while keeping the pocket doping constant, the tunneling width increases, thereby causing degradation in the injection mechanism. This leads to an increase in subthreshold swing, as shown in Fig.3.5,where the subthreshold swing at $I_D$ = 1 nA/$\mu$m and $V_D$ = 1 V is plotted as a function of pocket width.

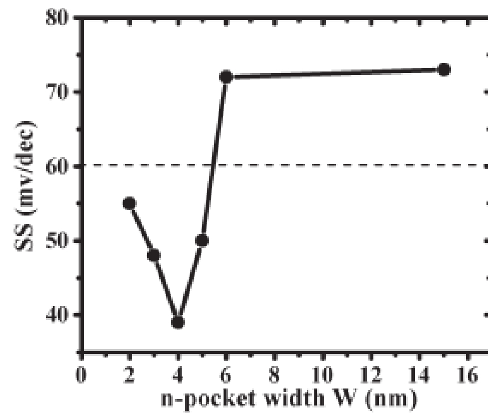


Figure 3.5: Subthreshold swing at $I_D$ = 1 nA/$\mu$m and $V_D$ = 1 V for different pocket widths.

Fig. 3.6 shows the relationship between pocket width and the doping concentration required to just fully deplete the pocket (referred to as $N_{\mathrm{DMAX}}$). The subthreshold swing of the device is seen to be a strong function of the pocket width (with concentration = $N_{\mathrm{DMAX}}$). As the pocket width increases, the tunneling width increases, reducing the sharpness of the electric field profile and degrading the subthreshold swing. The relationship observed at the chosen current levels (1 nA/$\mu$m and 100 nA/$\mu$m with $I_{\mathrm{OFF}}$ fixed at 10 pA/$\mu$m) is representative of the subthreshold regime. Below a pocket width of 6 nm, the subthreshold swing significantly drops below the conventional 60 mV/dec limit. Hence, in order to attain a subthreshold behavior with minimum possible swing, minimization of pocket width is essential.[4]

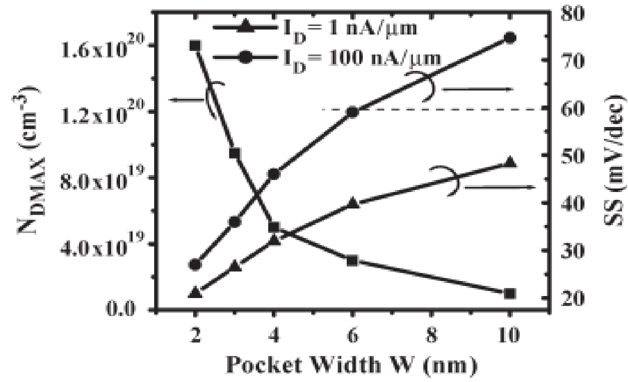


Figure 3.6 Doping required for just full depletion criterion and subthreshold swing at 1 nA/$\mu$m and 100 nA/$\mu$m (Doping × Width1.4 ≈ Constant)

### 3.5.3 Optimisation of channel length ($L_g$)

Fig. 3.7 shows the comparison of $I_{ON}/I_{OFF}$ ratio starting with same $I_{OFF}$ at $L_G$ = 100 nm. The PNPN n-MOSFET exhibits superior drive current capability as the channel length is scaled because the degradation in subthreshold swing (SS) and $I_{OFF}$ with scaling is much less. This is the result of a reduced source-to-channel coupling in the PNPN n-MOSFET because the built-in potential for a $p^+n^-$ (fully depleted) pn junction is small. In other words, the SCEs are greatly reduced. For $I_{OFF}$ = 1 nA/$\mu$m at $L_G$ = 100 nm, the $I_{ON}/I_{OFF}$ improvement at $L_G$ = 45 nm for the PNPN device is two orders more than the conventional SOI case. This is particularly beneficial for low standby power and low operating power technologies. Scaling the gate oxide thickness ($T_{OX}$) does not affect the source tunneling junction properties much and the only improvement is in $I_{ON}$, similar to that seen with $T_{OX}$ scaling in a normal MOSFET.[4]

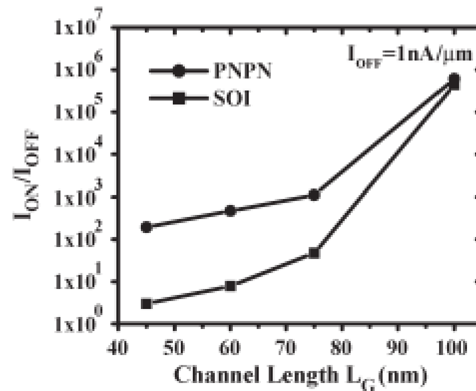


Figure 3.7 $I_{ON}/I_{OFF}$ ratio comparison for the PNPN and the conventional SOI n-MOSFET for the same $I_{OFF}$ = 1 nA/$\mu$m at $L_G$ = 100 nm. N-pocket width = 4 nm and $N_D$MAX = 5 × 1019 cm-3 for different $L$

## 3.6 DESIGN SPECIFICATION:

| PARAMETER NAME | PARAMETER VALUE | PARAMETER NAME | PARAMETER VALUE |
|---|---|---|---|
| $N_A$ (Source doping) | $1\times10^{20}$ $cm^{-3}$ | $L_g$ (Cavity length) | 30nm |
| $N_D$ (drain doping) | $1\times10^{20}$ $cm^{-3}$ | $t_g$ (gap thickness) | 9nm |
| $N_{CH}$ (channel doping) | $1\times10^{15}$ $cm^{-3}$ | $t_{sio2}$ (native oxide) | 1nm |
| $N_P$ (Packet doping) | $5\times10^{19}$ $cm^{-3}$ | $t_{ox}$ (oxide thickness) | 10nm |

## CHAPTER-4 SIMULATION RESULTS AND DISCUSSIONS

### 4.1 INTRODUCTION

In this chapter, all the simulation results and its discussion are briefly described for the double gate tunnel field effect transistor as a biosensor. The input characteristic of the device has been simulated. Also the characteristic of the device for neutral and charged biomolecule were also simulated. The threshold voltage, subthreshold swing and sensitivity has been calculated in this chapter.

### 4.2 SIMULATED STRUCTURE : PIN TFET

The difference between conventional TFET and proposed modified structure (PNPN TFET) is that the region between source and drain is covered with intrinsic silicon. The intrinsic concentration of silicon is $1.08\times10^{10}$ .The doping concentration concentration of source and drain is in order of greater than $10^{19}$. The conventional TFET is simulated as shown in fig4.1

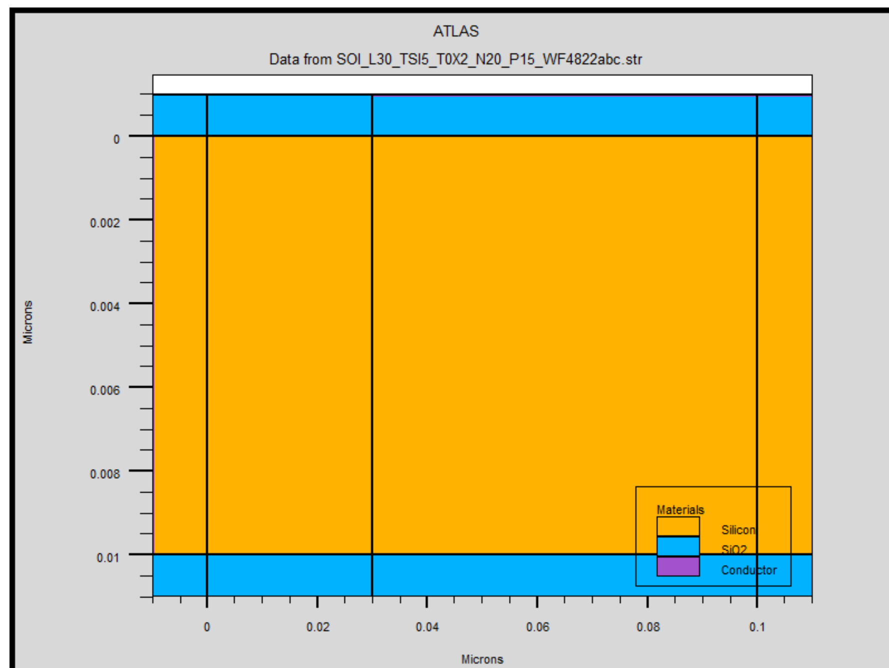


Figure 4.1 Simulated structure of pin TFET on silvaco Atlas

### 4.2.1 INPUT CHARACTERISTICS OF PIN TFET

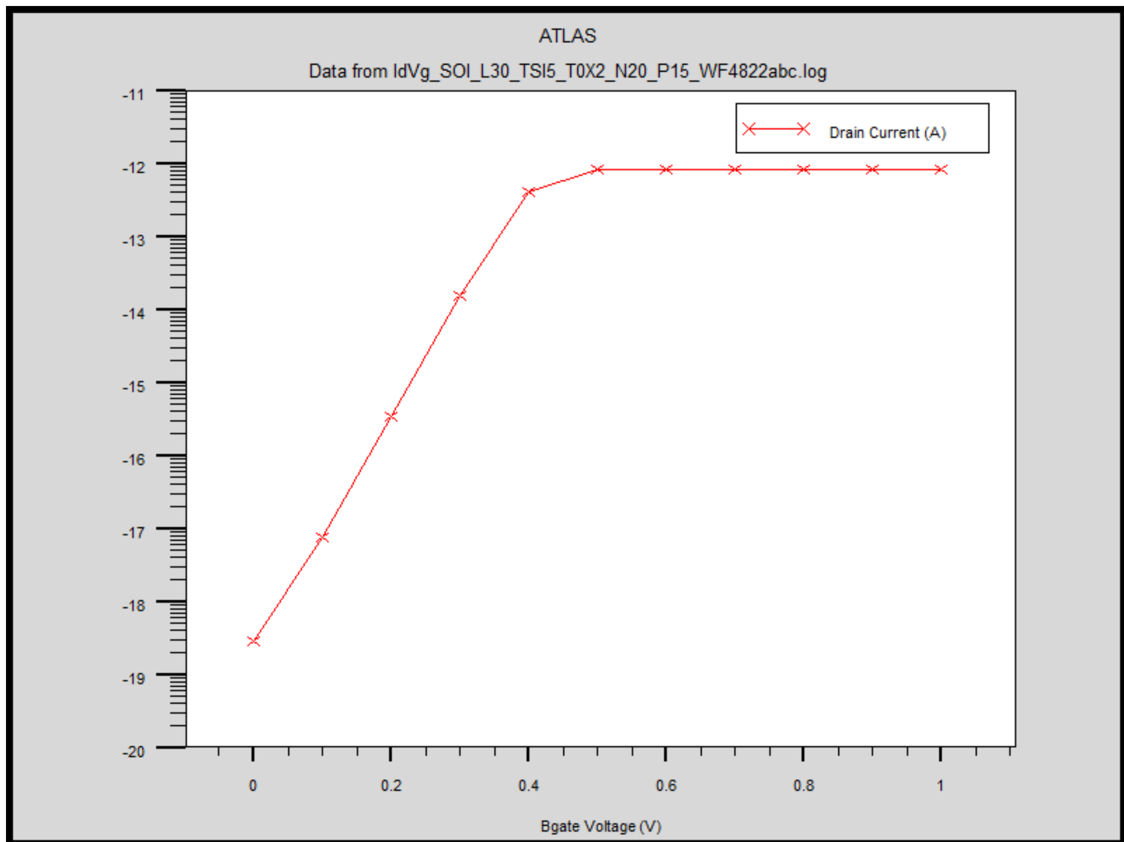


Figure 4.2 The Log ID versus Vgs characteristics of Pin TFET shows Ion current in the order of $10^{-11}$

The figure 4.2 shows the input characteristic for dissimilar drain voltage. It can be seen that Ioff current in the order of $10^{-18}$, which shows TFET is low power consumption device. There is a increase in the tunneling current, because in TFET tunneling current depends on the drain voltage also along with the gate voltage but. But beyond 0.6V of drain voltage there is not much improvement on the $I_{ON}$, due to the effect of the short channel effect (such as velocity saturation, DIBL and pinch-off mechanism).

## 4.3 SIMULATED STRUCTURE : PNPN TFET

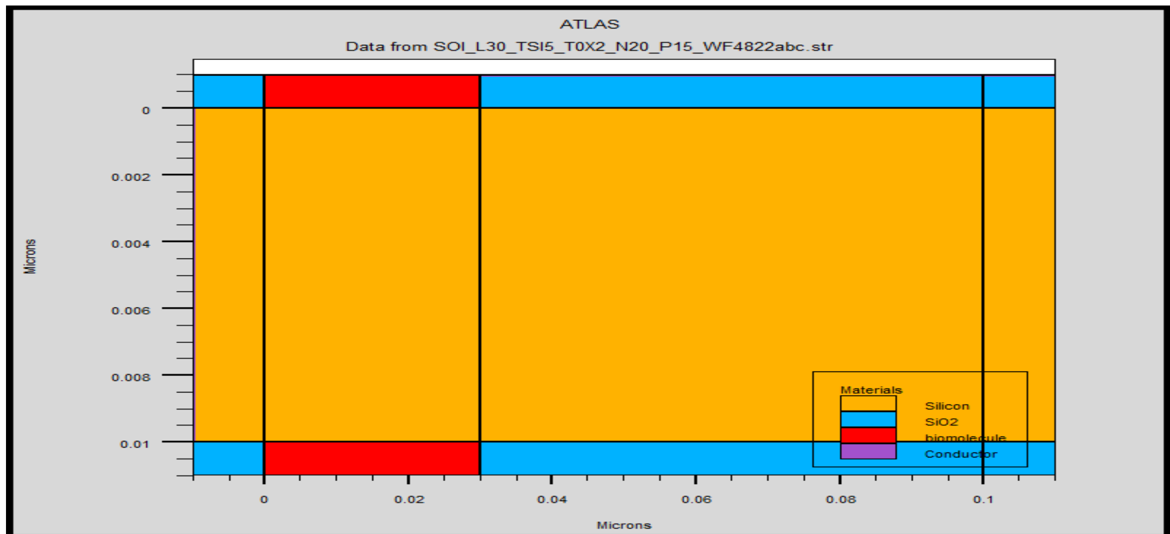


Figure 4.3 Simulated structure of PNPN TFET on silvaco Atlas

The proposed PNPN structure is simulated on silvaco atlas where red portion show cavity filled with biomolecule. Instead of an n+ source as in a conventional MOSFET, a tunneling junction formed between a p+ region and a narrow fully depleted n+ layer under the gate acts as a source of electrons for the channel. The thin fully depleted n+ layer reduces the tunneling width and increases the lateral electric field, thereby minimizing subthreshold swing as well as potential drop at the tunneling junction

### 4.3.1 INPUT CHARACTERISTICS OF PNPN TFET:

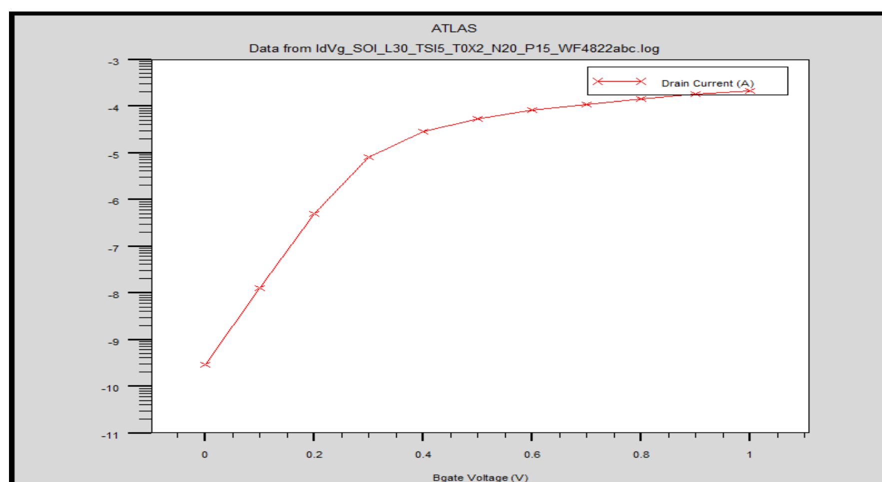


Figure 4.4 The Log $I_D$ versus Vgs characteristics of PNPN TFET shows Ion current in the order of $10^{-4}$

The Ion current in this device is in order of $10^{-4}$ which much more than PIN TFET which makes this device to be more attractive.

## 4.4 ENERGY BAND DIAGRAM OF TFET

Figure 4.5 shows energy-band diagram of the simulated device when it is in the OFF-state. Through this energy band diagram, it can be observed that the probability of tunneling of electrons is negligible when the device is in off state, as a large tunneling barrier exists in between the source and channel region.it will remain in this state because gate voltage is not sufficient to get desired band bending. Consequently in this state, the only current present is the p-i-n diode leakage current. But when the device is in ON state, as shown in the energy band diagram below (Figure 4.6), the tunneling barrier between the source and intrinsic are of the device lowers significantly, leading to a high possibility of tunneling of electrons from the valence band of the channel to the conduction band of the source.here applied voltage is sufficient enough to get desired band bending

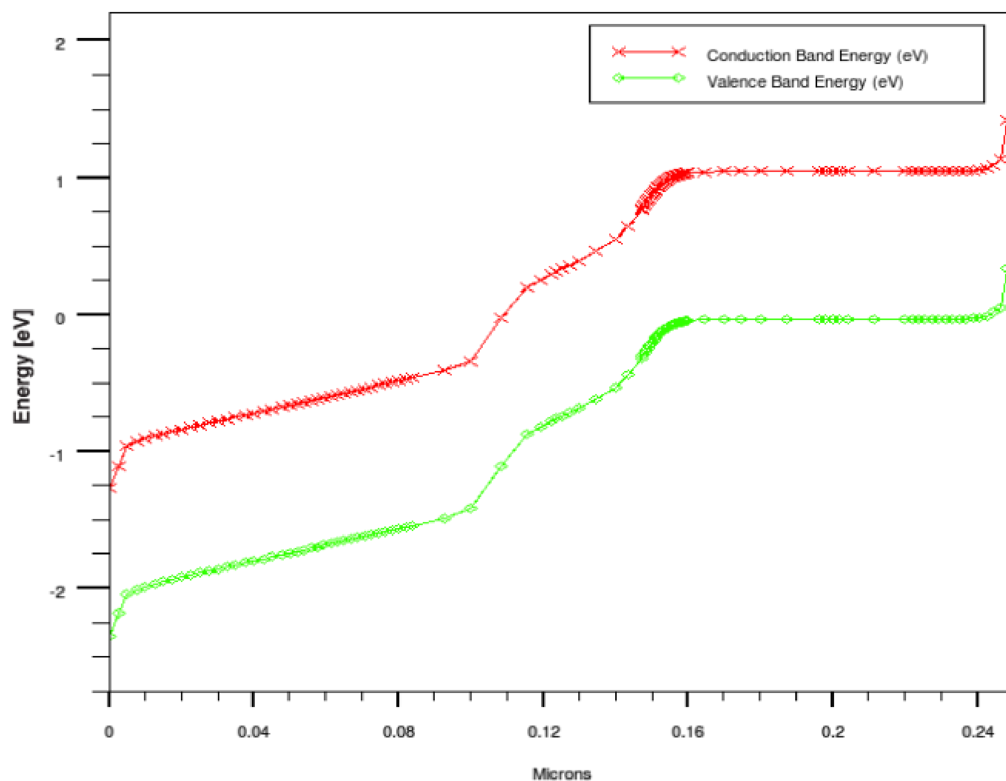


Figure 4.5 Energy band diagram of a device when it is off state

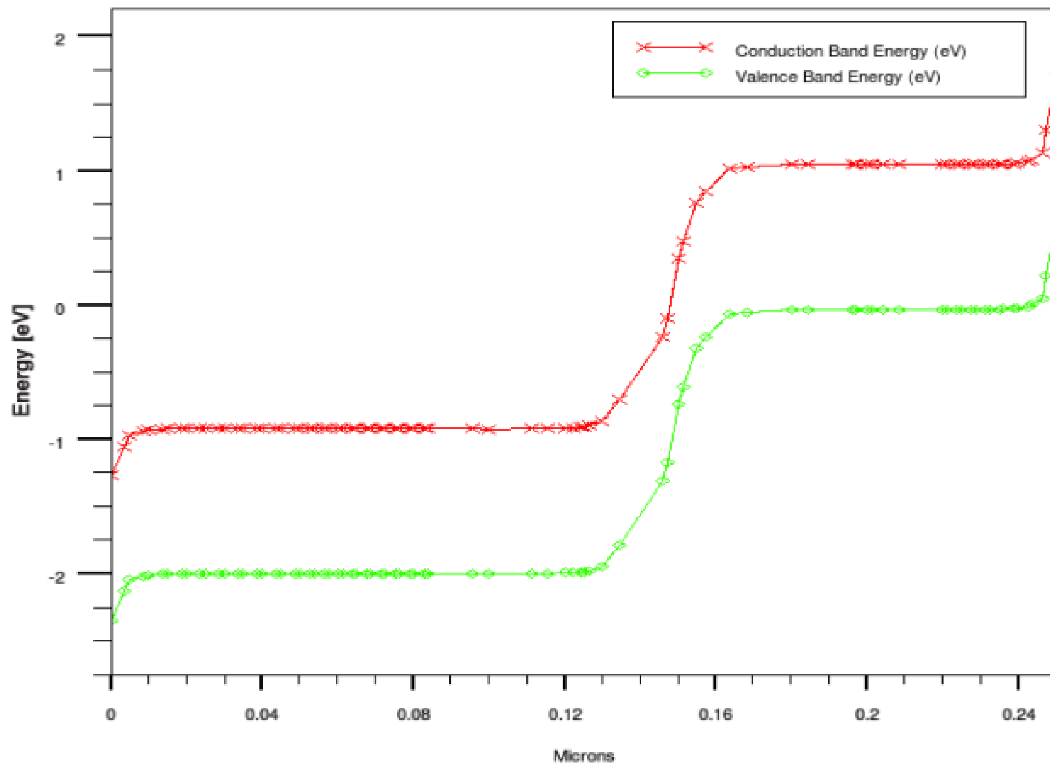


Figure 4.6 Energy band diagram of a device when it is ON state

## 4.5 DETECTION OF NEUTRAL BIOMOLECULE:

In this study, we focused on using the DMFET to detect the biotin–streptavidin system because it has one of the highest free energies of association for a non-covalent bond between a protein (streptavidin) and a small ligand (biotin) in aqueous solution. This biomolecule system is also useful in the diagnosis of certain diseases. The effect of neutral biomolecules is simulated by introducing different dielectric material having dielectric constant i.e., $K > 1$ because of biomolecules have their own dielectric constant as reported in literature streptavidin = 2.1, protein = 2.50, biotin = 2.63.

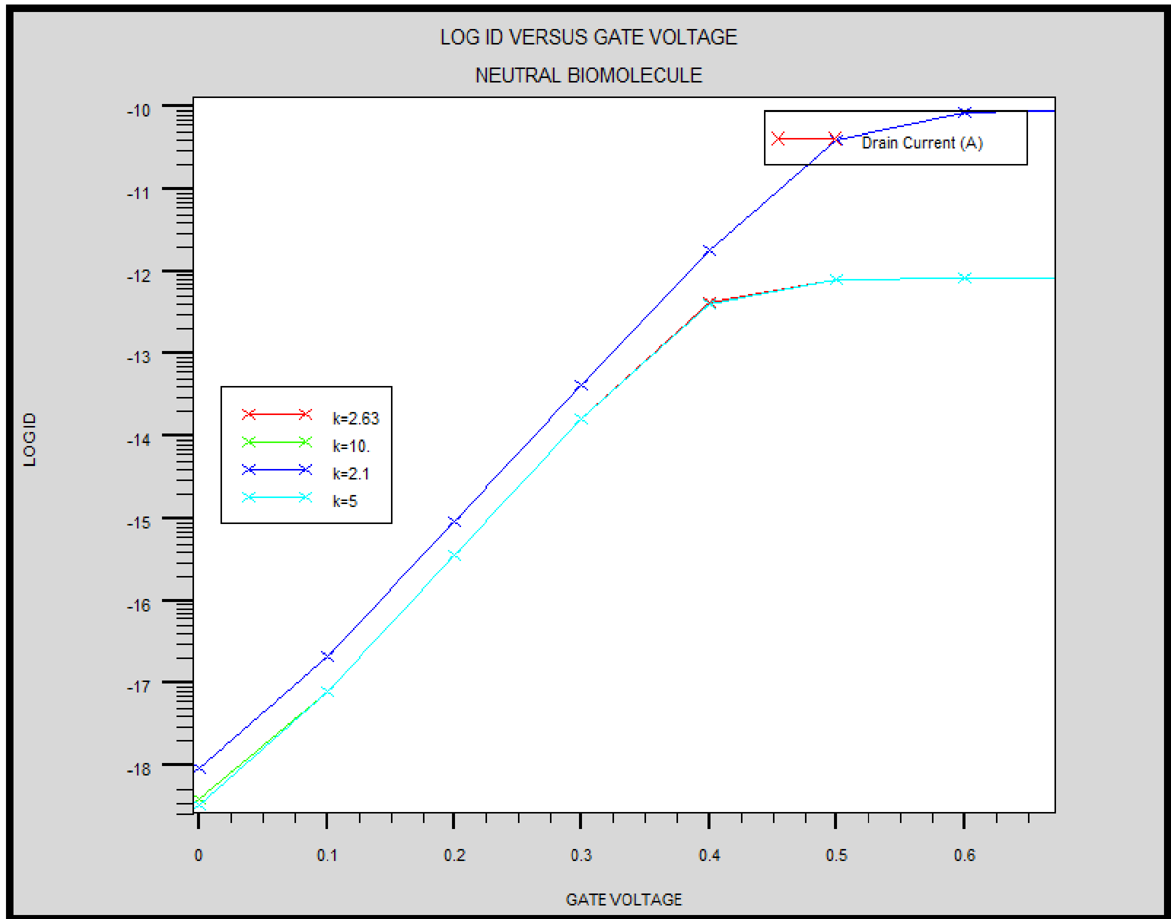


Figure 4.7 Log Id versus Gate voltage for different dielectric constant of biomolecule

The capacitance at the source side increases as the dielectric constant (of the biomolecule) in the nanogap cavity increases, resulting in additional band bending at the tunnel junction leading up to reduction in tunnel barrier width and, hence, increase in drain current. Also there is observation table which shows there variation in threshold voltage as well in subthreshold swing.

# TABLE NO. 4.1

| BIOMOLECULE NAME | DIELECTRIC CONSTANT(K) | CHANGE IN THRESHOLD VOLTAGE | SUBTHRESHOLD SWING(mv/decade) |
|---|---|---|---|
| Protein | 2.50 | 0.778 | 60.3384 |
| Biotin | 2.63 | 0.108 | 60.3381 |
| streptavidin | 2.1 | 0.070 | 60.3393 |
| APTES | 3.57 | 0.179 | 60.3368 |
| Air | 1 | 0 | 60.3410 |

From the table 4.1 we can observe that change in threshold increases when we increase the dielectric constant of neutral biomolecule. We can see this change in the fig.4.8

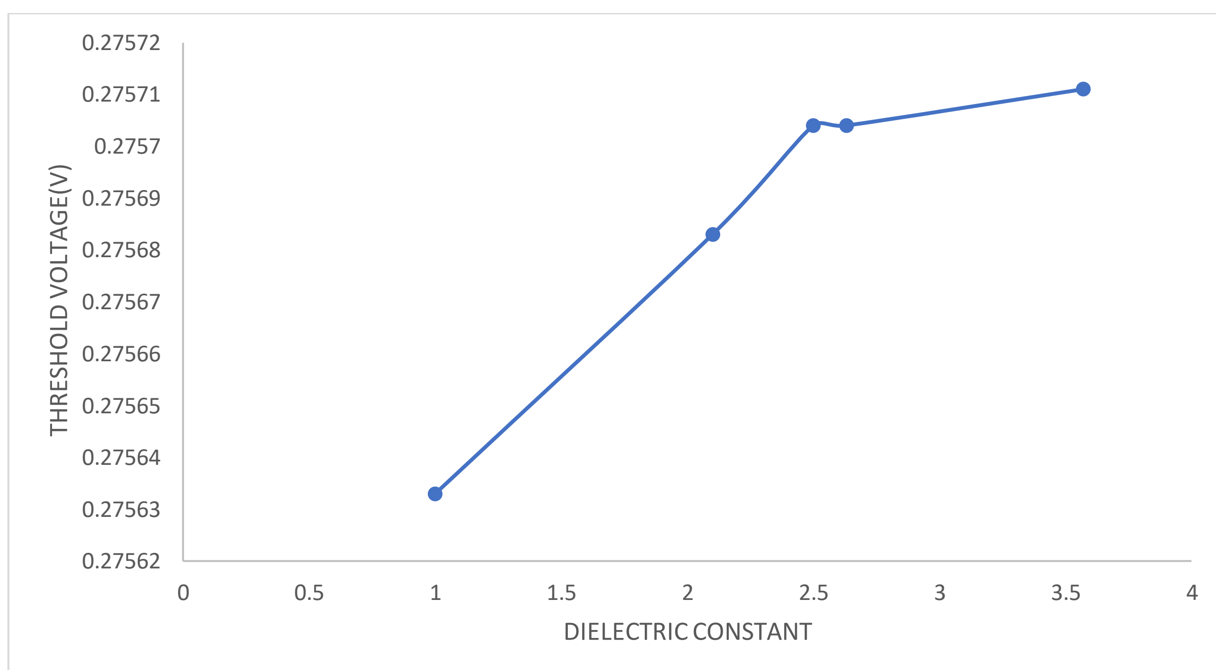


Figure 4.8 Threshold voltage versus dielectric constant variation

## 4.6 DETECTION OF CHARGED BIOMOLECULE

The effect of a charged biomolecule is emulated by introducing fixed oxide charges ($q_f$) in the dielectric layer. A single strand of DNA which is non hybridized possess both the dielectric constant as well as charge. The hybridization of DNA with its complementary strand leads to the increase in dielectric constant as well as charge due to increased phosphate groups, without any change in biomolecule layer. To simulate the effect of charge of the biomolecule negative or positive fixed charge at the cavity. Here detection parameter is Ion current which increases as we changes decreases the charge density in cavity of device.

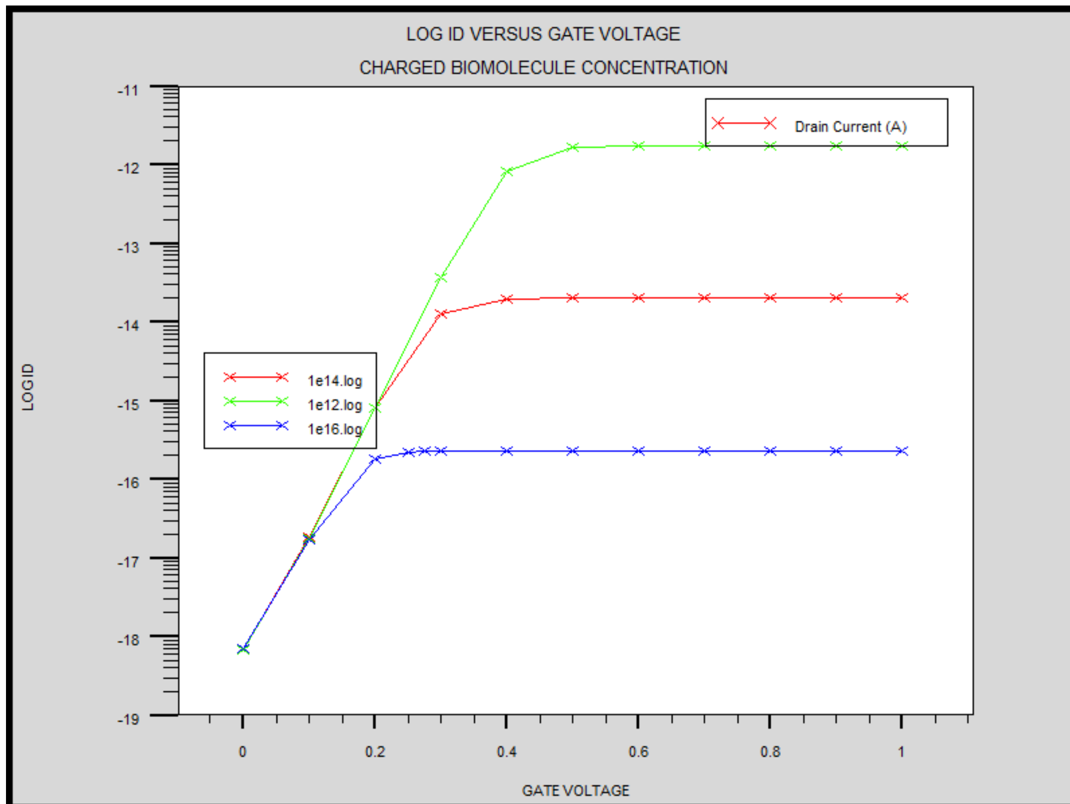


Figure 4.9 Log ID versus Vgs for charged biomolecule

# TABLE 4.2

| CHARGE DENSITY OF BIOMOLECULE ($m^2$) | THRESHOLD VOLTAGE (V) | CHANGE IN ION CURRENT (%) | SUBTHRESHOLD SWING (mv/decade) |
|---|---|---|---|
| $+5\times10^{20}$ | 0.381 | 84.8 | 56.1 |
| $-5\times10^{20}$ | 0.257 | 56.9 | 60.20 |
| $-5\times10^{11}$ | 0.2773 | 14.3 | 60.328 |
| $1\times10^{12}$ | 0.2708 | 75.4 | 60.41 |
| $-1\times10^{12}$ | 0.157 | 22.3 | 60.21 |

## 4.7 SENSITIVITY CALCULATION :

The mathematical formulation which has been considered to evaluate the sensitivity of n-type double gate TFET when the neutral and charged biomolecules are immobilized in the cavity is expressed as

$$\text{Sensitivity} = \frac{VTH(K=1)-VTH(K>1)}{VTH(K=1)} \text{ for neutral biomolecule}$$

$$\text{Sensitivity} = \frac{VTH(neutralbiomolecule)-VTH(charged\ biomolecule)}{VTH(neutral\ biomolecule)} \text{ for charged biomolecule}$$

Fig.4.10 gives sensitivity when neutral biomolecules are immobilized in the cavity regions of n-type double gate TFET. As the dielectric constant of the biomolecules present in the cavity region increases, the sensitivity for n-type double gate TFET linearly increases.

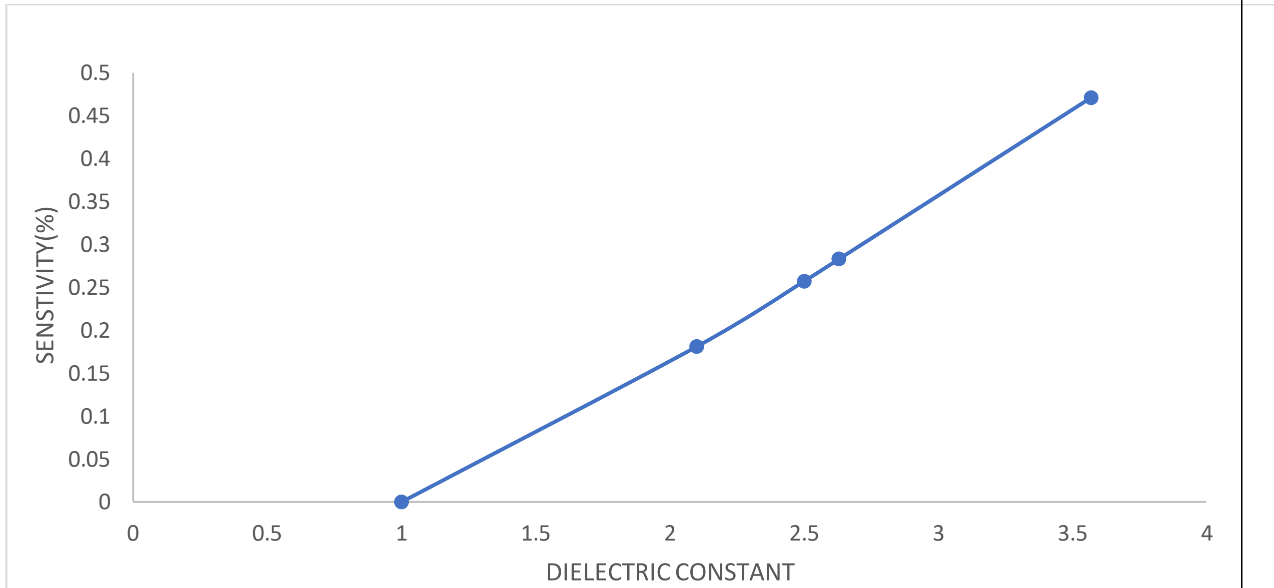


Figure 4.10 Sensitivity linear variation with dielectric constant of neutral biomolecule

As we can see sensitivity of device increases as dielectric constant of neutral biomolecule is increases, hence it shows good result in terms of sensitivity.

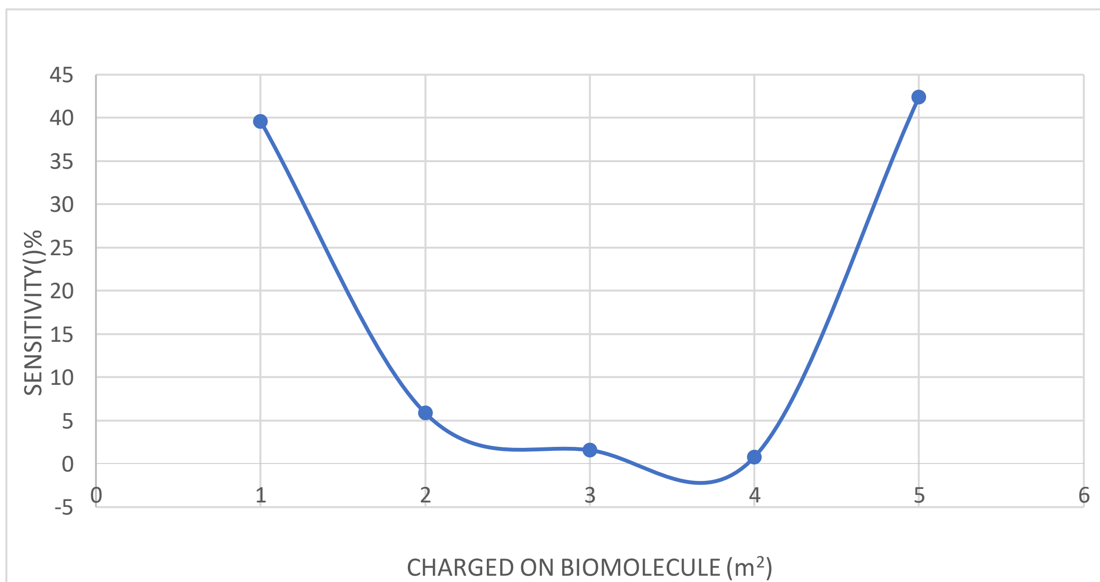


Figure 4.11 Sensitivity in parabolic pattern with respect to charged on biomolecule

The sensitivity decreases as negative charge on biomolecule increases but its shows increase in sensitivity as positive charge on biomolecule increases.

# CHAPTER 5 CONCLUSION AND FUTURE WORK

## 5.1 PERFOMANCE

The concept of a TFET-based biosensor has been proposed and analyzed for an array of biomolecule detection application (neutral, charged, hybrid). The p-n-p-n-based biosensor much better than PIN TFET biosensors in terms of its *I*on, providing steep SS and low leakage current. The low leakage current ensures low static power dissipation and thus enables the development of CMOS-compatible TFET-based low-power consumption circuitry for bio sensing applications.

The performance of the double gate TFET has been studied. satisfied results have been achieved for different performance parameters with the use of optimized device structure parameters, identified by the simulation studies of the impact of variations of different device parameters on the performance parameters of the PNPN TFET. The subthreshold slope for the device has been found to around 60.08mV/decade.

## 5.2 FUTURE WORK

In near future if successful hardware implementation will be possible it will completely change the scenario of CMOS biosensor circuit design. Low energy consumption, low power dissipation, low scale size really needed for the future design and fabrication of ICs so future research work and development should be done to develop this kind of sensor.

In coming it can provide big boost to health sector.

# REFERENCES:


1. http://en.wikipedia.org/wiki/MOSFET

2. Sneh Saurabh and M. Jagadesh Kumar, Senior Member, IEEE," Novel Attributes of a Dual Material Gate Nanoscale Tunnel Field-Effect Transistor", IEEE TRANSACTIONS ON ELECTRON DEVICES, VOL. 58, NO. 2, FEBRUARY 2011

3. TCAD silvaco user ATLAS manual

4. C.-H. Kim, C. Jung, H. G. Park, and Y.-K. Choi, "Novel dielectric modulated field-effect transistor for label-free DNA detection," *Biochip J.*, vol. 2, no. 2, pp. 127–134, Jun. 2008.

5. Dielectric Modulated Tunnel Field-Effect Transistor—A Biomolecule Sensor Rakhi Narang, *Student Member, IEEE*, Manoj Saxena, *Senior Member, IEEE*, R. S. Gupta, *Life Senior Member, IEEE*, and Mridula Gupta, *Senior Member,* IEEE ELECTRON DEVICE LETTERS, VOL. 33, NO. 2, FEBRUARY 2012

6. H. Im, X.-J. Huang, B. Gu, and Y.-K. Choi, "A dielectric-modulated field effect transistor for biosensing," *Nat. Nanotechnol.*, vol. 2, no. 7, pp. 430– 434, Jul. 2007.

7. J.-H. Ahn, S.-J. Choi, J.-W. Han, T. J. Park, S. Y. Lee, and Y.-K. Choi, "Double-gate nanowire field effect transistor for a biosensor," *Nano Lett.*, vol. 10, no. 8, pp. 2934–2938, Aug. 2010.

8. Analytical Model of Gate Underlap Double Gate Junctionless MOSFET as a Bio-Sensor Ajay1, Rakhi Narang2, Manoj Saxena3, and Mridula Gupta1 ,Third International Conference on Devices, Circuits and Systems (ICDCS'16)

9. S. Busse, V. Scheumann, B. Menges, and S. Mittler, "Sensitivity studies for specific binding reactions using the biotin/streptavidin system by evanescent optical methods," *Biosensors and Bioelectronics,* vol. 17, pp. 704-710, 2002.

10. J.-P. Colinge, C.-W. Lee, A. Afzalian, N. D. Akhavan, R. Yan, I. Ferain, P. Razavi, B. O'Neill, A. Blake, and M. White, “Nanowire transistors without junctions,” *Nature nanotechnology*, vol. 5, pp. 225-229, 2010.

11. C. Anghel, G. Hraziia, A. Gupta, A. Amara, and A. Vladimirescu, “30-nm tunnel FET with improved performance and reduced ambipolar current,” *IEEE Trans. Electron Devices*, vol. 58, no. 6, pp. 1649–1654, Jun. 2011.

12. The Tunnel Source (PNPN) n-MOSFET: A Novel High Performance Transistor Venkatagirish Nagavarapu, *Student Member, IEEE,* Ritesh Jhaveri, *Student Member, IEEE,* and Jason C. S. Woo, *Fellow, IEEE* TRANSACTIONS ON ELECTRON DEVICES, VOL. 55, NO. 4, APRIL 2008

13. L. De Michielis, L. Lattanzio, P. Palestri, L. Selmi, and A. M. Ionescu, “Tunnel-FET architecture with improved performance due to enhanced gate modulation of the tunneling barrier,” in *Proc. DRC*, Jun. 2011, pp. 111–112.

14. C. Ionescu-Zanetti, J. T. Nevill, D. Di Carlo, K. H. Jeong, and L. P. Lee, “Nanogap capacitors: Sensitivity to sample permittivity changes,” *J. Appl. Phys.*, vol. 99, no. 2, p. 024 305-5, Jan. 2006

15. TCAD Simulations of Double Gate Junctionless Tunnel Field Effect Transistor with Spacer Sapna Singh, Sudakar Singh Chauhan, (*Member IEE)*International Conference on Computing, Communication and Automation (ICCCA2017)

16. K. Boucart and A. M. Ionescu, “Double-gate tunnel FET with high-$\kappa$ gate dielectric,” IEEE Trans. Electron Devices, vol. 54, no. 7, pp. 1725–1733, Jul. 2007

17. W. Y. Choi, B.-G. Park, J. D. Lee, and T.-J. K. Liu, “Tunneling field-effect transistors (TFETs) with subthreshold swing (SS) less than 60 mV/dec,” *IEEE Electron Device Lett.*, vol. 28, no. 8, pp. 743–745, Aug. 2007.

18. E.-H. Toh, G. H. Wang, G. Samudra, and Y.-C. Yeo, "Device physics and design of double-gate tunneling field-effect transistor by silicon film thickness optimization," *Appl. Phys. Lett.*, vol. 90, no. 26, pp. 263507-1– 263507-3, Jun. 2007.

19. M. Jagadesh Kumar and Sindhu Janardhanan," Doping-less Tunnel Field Effect Transistor: Design and Investigation", IEEE TRANSACTIONS ON, ELECTRON DEVICES, Vol.60, No.10, pp.3285-3290, October 2013

20. Kathy Boucart and Adrian Mihai Ionescu," Double-Gate Tunnel FET using High-κ Gate Dielectric", ELECTRON DEVICES ,IEEE TRANSACTIONS ON, VOL. 54, NO. 8, JULY 2007

21. K. Gopalakrishnan, J. Plummer, and P. Griffin, "Impact ionization MOS device and circuitry simulations," Electronic Devices, IEEE Transactions on, vol. 53, no. 1, pp. 69–76, January 2005.